J. Membrane Biol. 154, 275–282 (1996)

The Journal of
Membrane
Biology

Clustered Distribution of Calcium Sensitivities: An Indication of Hetero-tetrameric Gating Components in Ca^{2+}-activated K^+ Channels Reconstituted from Avian Nasal Gland Cells

J.V. Wu, T.J. Shuttleworth, P. Stampe
Department of Pharmacology and Physiology, University of Rochester School of Medicine, Rochester, New York 14642

Received: 8 December 1995/Revised: 8 August 1996

Abstract. Calcium-activated potassium channels (maxi K^+ channels) isolated from avian nasal salt gland cells were reconstituted into lipid bilayers and characterized. The 266 pS channel is blocked discretely by charybdotoxin from the external solution at nanomolar concentrations and by Ba^{2+} from the cytosolic side at micromolar concentrations. Fast tetraethylammonium (TEA) block is seen as apparent reductions in amplitude of the unitary currents. From the extent of the reductions, TEA binding affinity was calculated to be 0.16 mM from the external solution and 37 mM from internal solution. The overall channel properties conform to those of maxi K^+ channels in other epithelial tissues. The calcium sensitivity of the channel was found to be variable from channel to channel, extending over a wide range of concentrations from 1 to 1,000 μM. Examination of the pooled calcium titration curves, revealed that these curves are grouped into five clusters, and the probability distribution of the clusters matches a binomial distribution. The Hill coefficient derived from the titration curves varies from 1 to 5 and is linearly correlated to calcium binding with a slope of 1 per 10-fold change in K_d. Clustered titration curves with such a characteristic suggest that the gating components and the calcium binding sites of the maxi K^+ channels in the avian nasal gland are hetero-tetrameric and may result from random mixing of two distinct subunits possessing high and low calcium sensitivities, respectively.

Key words: Salt gland — Epithelium — Lipid bilayer — Potassium channel — Ca^{2+}-activated K^+ channel — Calcium sensitivity

Correspondence to: P. Stampe

Introduction

Large conductance Ca^{2+}-activated potassium channels (maxi K^+ channels) are identified by a large unitary conductance, voltage dependence, charybdotoxin (CTX) blockade, and the signature Ca^{2+}-dependent activation. The sensitivity of the latter, commonly described by a calcium concentration ($[Ca^{2+}]$) at which the open probability reaches 0.5, varies from tissue to tissue in the range of 0.01 μM to 100 μM (McManus, 1991). Even in the same tissue under identical experimental conditions, three- to fivefold changes in this sensitivity are observed from channel to channel, while permeation behavior remains indistinguishable (Moczydlowski & Latorre, 1983). Similar diversity of calcium sensitivities seen in patch clamp recordings (Richards et al., 1989) suggests that this variability does not result from any possible artifacts introduced during the isolation and reconstitution process, but is more likely related to the native structure of the channels.

Recent progress in the analysis of maxi K^+ channels using site-directed mutagenesis has revealed the possible molecular basis for the heterogeneity of maxi K^+ channels. The tetrameric formation of the maxi K^+ channel was revealed by the TEA blocking behavior of the maxi K^+ channels expressed by a mixture of RNAs which encode two distinct TEA binding affinities (Shen et al., 1994). Such a hetero-tetrameric pore construction diversifies the permeation and block properties that associate with a pore. Similarly, if the gating components of a maxi K^+ channel are tetrameric, in principle it should be able to produce the observed variable calcium sensitivities, provided that subunits with different calcium sensitivities are expressed in a cell. The latter condition is confirmed by the reports in which the C-terminal alternatively spliced variants of *slo* channels exhibited different calcium sensitivities (Tseng-Crank et al., 1990; La-

grutta et al., 1994). Variability in calcium sensitivity may also arise from the relative phosphorylation and dephosphorylation of the selected subunits (Egan et al., 1993; Reinhart & Levitan, 1995). Given that the site of calcium activation is confined to a distinct domain at the C-terminal that is independent of the permeation properties (Wei et al., 1990), for the above idea to be valid, it is necessary to establish whether the gating components themselves are hetero-tetrameric.

Avian nasal exocrine glands are an extra-renal salt excretory tissue. They produce a NaCl-rich fluid via a mechanism apparently identical to that seen in the acinar cells of more traditionally studied exocrine tissues (Ernst & Ellis, 1969) but without the usual complications seen in such tissues where ionic secretion often operates in parallel with the secretion of enzymes and mucus or simultaneously with ion absorption (Shuttleworth & Thompson, 1989). Upon elevation of cytosolic Ca^{2+} concentration as a result of the action of appropriate neurotransmitters and hormones, two types of Ca^{2+}-activated conductance pathways are seen (Petersen, 1986; Martin & Shuttleworth, 1994). In the basolateral membrane, the activated maxi K^+ channels allow K^+ release to the blood side, whereas in the apical membrane the activated Cl^- channels transport Cl^- to the lumen. Effectively, these calcium-activated pathways operate together with a Na^+-K^+-$2Cl^-$ cotransporter and Na^+-K^+ pump to produce an electrogenic transepithelial Cl^- transport. To further understand the physiological role of maxi K^+ channels in secretion, detailed knowledge of this pathway at the single-channel level is needed. Using the patch clamp technique, Richards et al. (1989) were able to record and analyze the unitary current of this channel, and found variation in calcium sensitivities. In the present study, avian nasal gland maxi K^+ channels were isolated and reconstituted into lipid bilayers. With the consequent advantage of being able to record for prolonged duration and independently perfuse both sides of the membrane, we have been able to examine the Ca^{2+} sensitivity of this channel at a higher resolution. We found that calcium titration curves are grouped into five distinct clusters, suggesting a heterotetrameric construction of gating components in these channels. Preliminary data of this finding have been reported in an abstract form (Wu et al., 1996).

Materials and Methods

Vesicle Preparation

Ducklings of 6–10 days old (Ridgeway Hatcheries, La Rue, Ohio) were euthanized after feeding 1% NaCl drinking water *ad libitum* for 48 hr to induce differentiation of the secretory cells. Supraorbital nasal salt glands were injected *in situ* with 1 ml/gland of ice-cold saline to remove red blood cells (Shuttleworth & Thompson, 1989), and then immersed in ice-cold buffer (150 mM NaCl, 10 mM MOPS, and 5 mM EGTA, pH 7.4). Immediately after the addition 1 μg/ml of phenylmethylsulfonylfluoride (PMSF), the glands were homogenized with a Tekmar Tissuemizer for 25 sec, then transferred to a Wheaton homogenizer and ground on ice for 10 times (loose pestle), and then 40 times (tight pestle). The homogenate was centrifuged in a Beckman GS-15R at 10,000 rpm (8700 × *g*) using a F0630 rotor for 10 min at 4°C. The supernatant obtained was layered on top of a step gradient of sucrose (34, 26 and 20%) in 10 mM MOPS pH 7.4 and centrifuged at 25,000 rpm (38000 × g) using a SW27 rotor in a Beckman L5-75 Ultracentrifuge, for 60 min at 4°C. The membrane fraction lying at the 20 and 26% interface was extracted with a syringe and transferred to a centrifuge tube with three volumes of distilled water. Following centrifugation at 40,000 rpm (146,000 × *g*) using a 50.2 TI rotor for 60 min, the pellet was resuspended in isotonic sucrose buffer (250 mm sucrose and 10 mM MOPS, pH 7.4), frozen on dry ice, and stored at −70°C.

Planar Bilayers and Channel Insertion

The bilayer recording chamber was built from a block of acetyl copolymer (Patriot Plastics). It consists of a 250 μm pin hole drilled through a thin wall which separates *CIS* and *TRANS* reservoirs. On the day of the experiment, two volumes of lipid 1-palmitoyl, 2-oleoyl-phosphotidylethanolamine/1-palmitoyl, 2-oleoyl-phosphatidylcholine (10 mg/ml; PE/PC, 7:3, Avanti Polar Lipid) were dried with N_2 and redissolved in one volume of *n*-decane (Sigma). The pin hole was prepainted with the lipid solution and allowed to dry for >10 min before the *CIS* solution (650 mM KCl, 10 mM HEPES, 100 μM Ca^{2+}, pH 7.4) and the *TRANS* solution (50 mM KCl, 10 mM HEPES, 100 μM Ca^{2+}, pH 7.4) were added to the reservoirs. Membrane vesicles, 10–15 μl, were pipetted into the *CIS* side of the chamber which was continuously stirred by a small magnetic bar. More than 95% of insertions under these conditions resulted in the Ca^{2+}-sensitive side facing the *CIS* reservoir, and only channels inserted in this orientation were used for recordings. We therefore subsequently refer to the *CIS* reservoir as the internal side and the *TRANS* reservoir as the external side. After incorporation of a single channel, the *CIS* side was washed with isotonic 150 mM KCl, 10 mM HEPES, pH 7.4 and the *TRANS* side was replaced with 150 mM KCl, 100 μM Ca^{2+}, 10 mM HEPES pH 7.4, to stop further fusion. Stock Ca^{2+} solution (100 μM or 10 mM Ca^{2+}) was then added to the internal solution to obtain the desired Ca^{2+} concentration from 1 to 500 μM. Internal solutions with free Ca^{2+} concentration below 1 μM were made with EGTA-Ca^{2+} buffers containing (in mM): 150 KCl, 10 HEPES, 5 EGTA, plus 4.28 $CaCl_2$ (for 1 μM free Ca^{2+}), 3.74 $CaCl_2$ (for 0.5 μM Ca^{2+}), and 2.98 $CaCl_2$ (for 0.25 μM free Ca^{2+}), pH 7.4. Stock solutions of charybdotoxin (CTX), $BaCl_2$, and tetraethylammonium (TEA) were prepared, and pipetted into the chamber to produce the desired concentrations when needed.

Data Acquisition and Analysis

Currents were recorded using an Axopatch 200A patch clamp amplifier (Axon Instruments, Foster City, CA) in capacitive feedback configuration and a lowpass cutoff filtering frequency of 1 kHz. The analog output signal was digitized by a Data Acquisition Processor (DAP 3200e, Microstar Laboratories) at 100 kHz. Open and closed times were computed by an on-board processor (486DX) on-line at 100 kHz with a threshold set to 50% of the whole open-level current. At the same time, single-channel currents were sampled at 2 kHz. Cumulative open probability (P_o) was computed from the total open and closed time of 2–10-min recording. During the recording, P_o *vs.* number of transitions was displayed after every 1,000 transitions and the stability

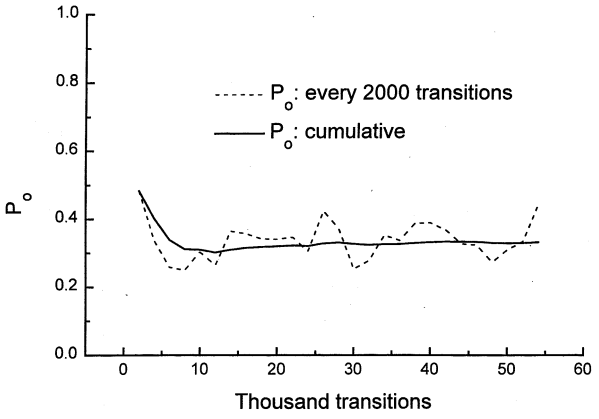

Fig. 1. Stabilization of cumulative open probability. The averaged open probability at the end of each 2,000 transitions (broken line) and cumulative open probability (solid line) are plotted against number of transitions. The total duration of the recording is about 7 min.

of P_o was continuously monitored. In most cases P_o reached a steady state in about 1 min. A typical plot with a total duration of ~7 min is shown in Fig. 1. The averaged open probability for each 2,000-transition interval shows considerable fluctuations. On the other hand, the cumulative open probability stabilized in a few minutes. Only 1 out of 30 recorded channels showed irreversible shift from high Ca^{2+} sensitivity to a lower one and it has thus been excluded from analysis. A Pentium/60 MHz Personal Computer and a custom-written program were employed to control the experiment, store data on a hard drive, and analyze the data. During off-line analysis, all-point amplitude histograms were constructed and the single-channel amplitude was obtained through least-squares fit of peaks using Gaussian distributions.

Results

Characterizations of Avian Nasal Gland Maxi K^+ Channels

Figure 2*A* illustrates the unitary currents of a maxi K^+ channel recorded in symmetrical 150 mM KCl, 100 μM Ca^{2+} solutions at three voltage levels. The current amplitudes at seven voltages were analyzed with all-point histograms and least-squares fit of Gaussian distributions, resulting in the *I-V* relationship shown in Fig. 2*B*. To obtain the unitary conductance, the data points were linearly fitted, yielding a slope conductance of 266 pS shown as the solid straight line. Open probability of this channel *vs.* transmembrane voltage was calculated from open- and closed times with a criterion set at one-half the whole amplitude of the unitary current. The data points at discrete voltages were least-squares fitted with the Boltzmann distribution shown as a solid curve (Fig. 2*C*). Two parameters were derived from the fitting. $V_{0.5} = -15$ mV represents the half-activation voltage and $V_{e\text{-fold}} = 9.5$ mV is the voltage sensitivity, i.e., a voltage difference needed to produce an *e*-fold change in open probability.

Blockage of the channel by CTX is discrete as shown in Fig. 3*A*, where the outward currents were recorded in symmetrical 150 mM KCl, 100 μM Ca^{2+} solutions and the internal surface of the membrane was held at +30 mV. The top two traces are control recordings at two different time scales, whereas the bottom trace shows a 200-sec trace in the presence of 10 nM external CTX. From 152 min of recorded data, the open-time constant $\tau_o = 0.87$ sec and the closed-time constant $\tau_c = 26.7$ sec were computed, which corresponds to an on-rate constant $k_{on} = 8.7 \times 10^8$ sec^{-1} M^{-1} and an off-rate constant $k_{off} = 3.8 \times 10^{-2}$ sec^{-1}, respectively. These data indicate a CTX equilibrium dissociation constant $K_d = 3.2$ nM. In Fig. 3*B*, an example of the discrete internal barium block is shown. In this case, the off-rate constant was estimated to be 6.3 sec.

Unlike CTX and barium blockade, TEA binding was too fast to be discretely resolved and consequently is displayed as a reduced unitary current. The recorded current in control experiments, and those following either external or internal TEA block are shown in Fig. 4. In the presence of 0.1 mM external TEA, the current was reduced to 61.7% of the control, whereas internal application of 20 mM TEA produced a reduction of 64.9% of the control. These reductions in amplitude were derived from histogram analysis and the least-squares Gaussian fit. Assuming a one-to-one blocking stoichiometry, the equation $(I_{control} - I_{block})/I_{control} = [TEA]/([TEA] + K_D)$ was used to calculate the equilibrium binding constant, which is $K_D = 0.15$ mM from the external side and 37 mM from the internal side. The discrete open probability measured by the threshold-crossing method showed no appreciable changes in the presence of TEA on either side.

Clustered Distribution of Calcium Sensitivities

One of the important aspects of the channel characterization was to determine the calcium sensitivity of avian nasal gland maxi K^+ channels. We did this by measuring the open probability with stepwise increases in the internal free calcium concentration. The calcium sensitivity was found to vary considerably from channel to channel. We illustrate this variation in Fig. 5 by showing the raw unitary currents of four different channels at the same internal free $[Ca^{2+}]$ of 5 μM. Differences in the open probability are clearly visible. To evaluate the variations in a systematic way, we carried out a series of experiments and pooled all 29 titration curves in one graph shown in Fig. 6. As can be seen, the curves are widely spread but not uniformly distributed. Simple visual inspection indicates they are grouped into five clusters.

To manifest the clustered distribution further, we

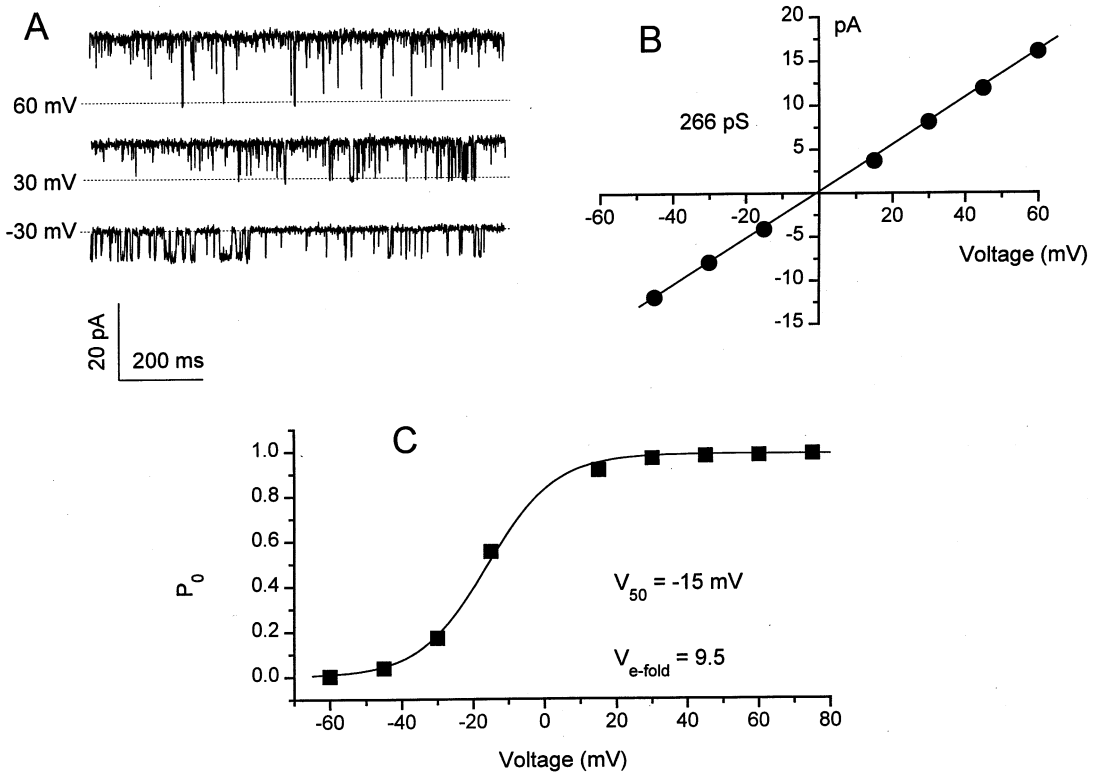

Fig. 2. Voltage dependence of the single-channel current and the open probability of a nasal-gland maxi K^+ channel reconstituted into a planar lipid bilayer. All the currents were recorded in symmetrical 150 KCl solutions with 100 μM calcium. (*A*) Single-channel currents at three different voltages. The broken lines are the current where the channel is closed. (*B*) The voltage dependence of the unitary current amplitude of the channel. (*C*) The voltage dependence of the open probability of the channel. The solid line represents a least-squares fit of the Boltzmann distribution, $P_o = P_{max}/\{1 + \exp[-V-V_{1/2})/d]\}$, where d is the voltage sensitivity in mV per e-fold change in open probability.

transformed each P_o (excluding values above 95%) at a given $[Ca^{2+}]$ to an apparent K_d according to the equation $K_d = [Ca]/\{P_o/(1 - P_o)\}^{1/h}$, where h is a constant. All the K_d's were then binned and plotted in Fig. 7. We tried several h values ranging from 1.8 to 2.8 to examine the corresponding histograms, and found no significant changes in their general five-peak feature. Setting h = 2.3, to typically show the data, is thus rather arbitrary. The histograms in Fig. 7 were least-squares fitted with five Gaussians plotted as solid curves. Using this fitted Gaussian curve, we estimated the variance of the histogram which gives a standard deviation $\sigma_{fluctuation} = 1.0$. To quantitatively evaluate the clustering, the histogram was least-squares fitted with a single Gaussian, as if the histogram is extensively low-pass filtered or averaged to approximately represent the least clustered distribution. From this curve and the peaks and wells of the multi-peak Gaussian fit, we obtain a clustering related standard deviation $\sigma_{clustering} = 3.2$. The ratio of these two standard deviations, analogous to the concept of ''signal-to-noise ratio,'' shows that the clustering induced deviation is over three times more prominent than that of the fluctuations. From the area ratio under the curve of each Gaussian and that of the summed Gaussians, we calculated the probability of each point falling into one of the five groups, which was 0.087, 0.26, 0.52, 0.23, and 0.11 (starting from the low K_d), respectively.

The apparent segregation of these groups allowed us to average data within each group, and the resulting averages are plotted in Fig. 8. These averaged points were least-squared fitted with the Hill equation $P_o = P_{max}/\{1 + (K/[Ca]^H\}$ (Hill, 1922) and the results were plotted as the solid curves. The fitted apparent equilibrium binding constants and Hill coefficients are all listed in the lower inset of Fig. 8. To examine the dependence of these parameters, we plotted them in the upper inset. H *vs.* K_d follows an apparent linear relation and gives a slope of about one per 10-fold change in $[Ca^{2+}]$ concentrations.

Discussion

This study reports the findings of experiments where the maxi K^+ channels of the avian nasal gland have been isolated and reconstituted into lipid bilayers. With the advantage of being able to accurately control the solutions on both sides of the channel and recording single channel current for prolonged duration, we have characterized the maxi K^+ channels in this tissue and revealed a detailed feature regarding calcium activation that may have significant structural implications.

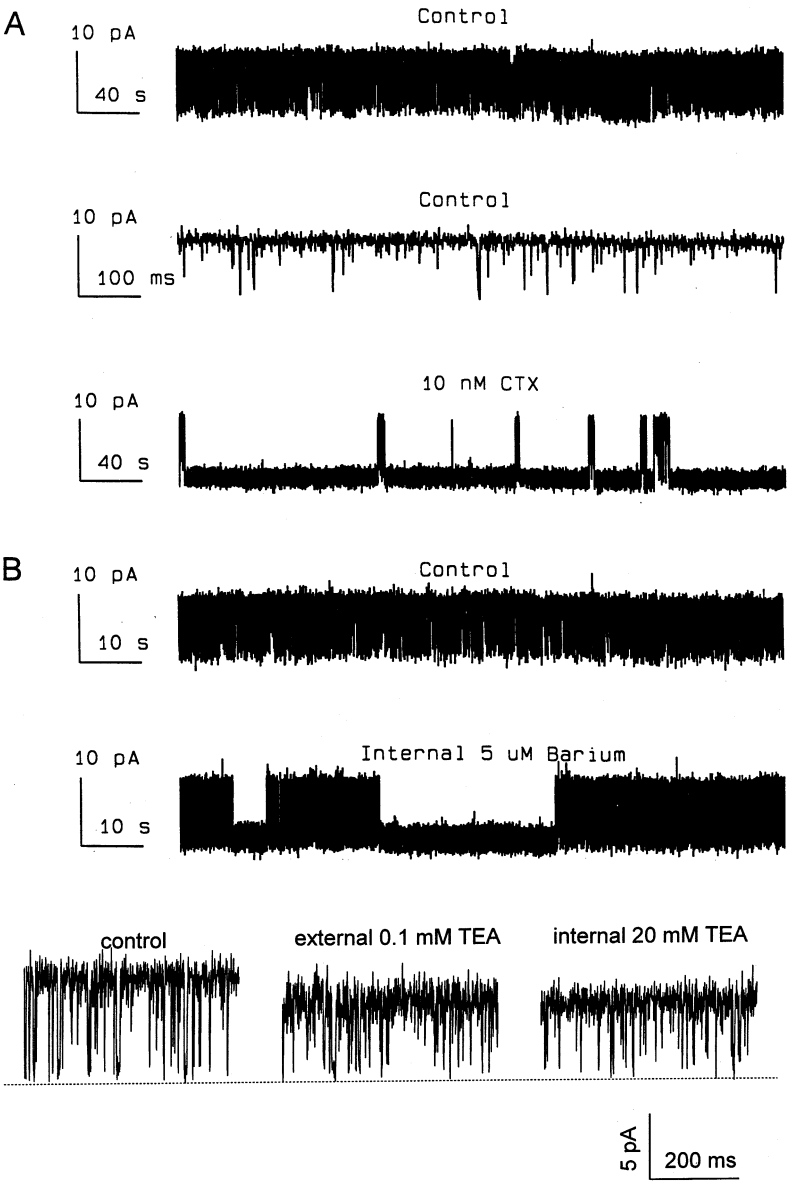

Fig. 3. (*A*) Blockage of a single nasal gland maxi K^+ channel with charybdotoxin (CTX). *Top and middle:* Control single-channel current in symmetrical 150 mM KCl solutions with 100 μM calcium at 30 mV. *Bottom:* Discrete block of the current following external application of 10 nM CTX. (*B*) Channel block by barium. *Upper:* Control unitary current in the symmetrical 150 mM KCl solutions at 30 mV. *Lower:* Discrete block of the current in the presence of 5 μM barium in the internal (*CIS*) side of the chamber.

Fig. 4. Fast block of a single maxi K^+ channel by tetraethylammonium (TEA). *Left:* Control single channel current in symmetrical 150 mM KCl solutions with 100 μM calcium at 30 mV. *Middle:* The current recorded with 0.1 mM TEA in the external (*TRANS* chamber) solution. *Right:* With 20 mM TEA in the internal solution (*CIS* chamber). The broken line represents the closed level of the current.

Comparison with Maxi K^+ Channels from Other Epithelia

The open channel properties and the gating behavior of this channel characterized by a large unitary conductance and Boltzmann type voltage dependence conform to those of maxi K^+ channels found in many tissues (Lattore & Miller, 1983). The unitary conductance of 266 pS in symmetrical 150 mM K^+ solutions is consistent with that found in gallbladder (Segal & Reuss, 1990) and oviduct epithelium (James & Okada, 1994), the principal cells of the cortical collecting duct (Schlatter et al., 1993), and sweat gland cells (Henderson & Cuthberg, 1991), but is about 20% higher than that in a previous study done in the same cell type using patch clamp techniques (Richards et al., 1989).

The CTX, TEA, and Ba^{2+} block of this channel are quantitatively similar to those found in mammary cells (Furuya et al., 1989), avian salt gland (Richards, 1989), gallbladder (Segal & Reuss, 1990), cortical collecting duct (Schlatter et al., 1993), distal colon (Turnheim et al., 1989), and choroid plexus (Brown, Loo & Wright 1988) epithelia. From these similar characteristics, we conclude that the maxi K^+ channels found in avian nasal gland cells are not significantly different from those found in a variety of other epithelia.

Distribution of Calcium Titration Curves

One of our goals was to evaluate the role of this channel under physiological calcium concentrations. We did this

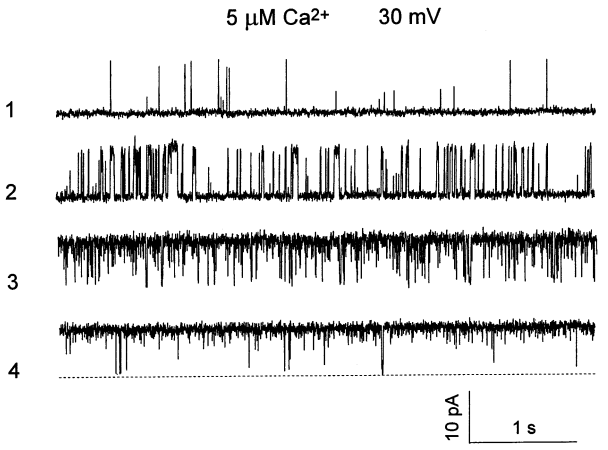

Fig. 5. Heterogeneous calcium sensitivities of maxi K^+ channels isolated from the same tissue in response to the same calcium concentration. Single-channel current of four individual channels recorded at the same calcium concentration and voltage conditions. The broken line represents the closed level.

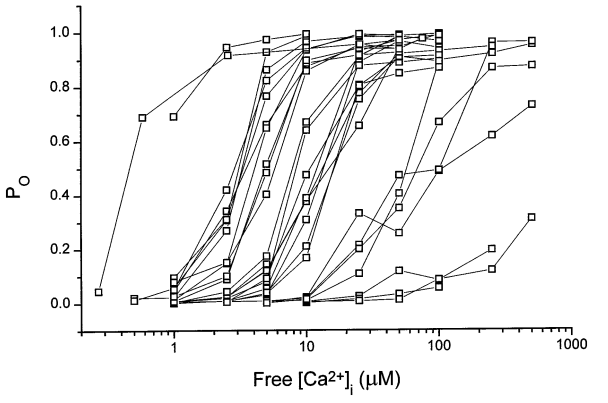

Fig. 6. Clustered distributions of calcium sensitivities. The open probabilities of 29 channels in a series of experiments are plotted against internal free calcium concentration in logarithmic scale. Each symbol represents an individual measurement and recordings from the same channel are connected with a solid line.

by characterizing the calcium dependent activation of the channel and found that not only are the calcium sensitivities generally outside the normal cytosolic calcium range of concentrations even at +30 mV, they also vary widely depending on the individual channel. Since similar variability has been found earlier in the same tissue using the patch-clamp technique (Richards et al., 1989), possible artifacts introduced by the isolation and reconstitution process can be discounted and this suggests that the source of the observed variability is likely to be related to some component of the structure of the channel.

Upon quantitative analysis of calcium titration curves, we found that the Hill coefficient *vs.* the calcium sensitivity K_d follows a linear relation with a slope of about 1 per 10-fold change in $[Ca^{2+}]$. This dependence

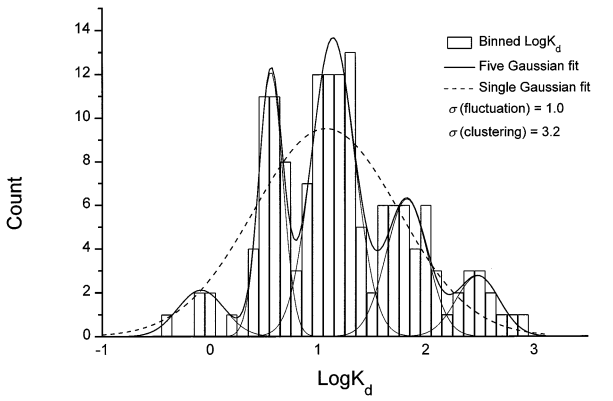

Fig. 7. Histogram illustration of clustering Ca^{2+} sensitivity. Each P_o in Fig. 6 is transformed to K_d through a function $K_d = [Ca]/\{P_o/(1 - P_o)\}^{1/h}$ with $h = 2.3$ set as constant. All the calculated K_ds were binned with a bin width of $\log_{10}\Delta Kd = 0.1$ and plotted as vertical open bars. The histogram is least-squares fitted with multiple Gaussians shown as solid curves and with single Gaussian represented by the broken line.

shows clearly that increases in calcium sensitivity are associated with increases in channel Ca^{2+} binding cooperativity. One possible explanation for this observation is an increase in the number of binding sites. Furthermore, if the Hill coefficient reflects the minimum number of cooperative ligand binding sites on a receptor (Adair, 1925), we estimate that there are as many as five or more possible Ca^{2+} binding sites on the channels isolated from this tissue. The detailed linking mechanism however needs more elaborate analysis. It is well known from the literature that Hill coefficients summarized from different preparations can vary as much as from 1 up to 6 (*see* McManus, 1991, for review). Our observed variation in the channels derived from the *same native tissue* has not previously been reported. In addition we found a linear correlation between the Hill coefficient and K_d.

In a study of two large-conductance Ca^{2+}-activated K^+ channels from Drosophila (dslo) and human (hslo) expressed in *Xenopus* oocytes, a Hill coefficient of 1.9 was calculated for both channels (DiChiara & Reinhart, 1995). These values obtained from macroscopic currents are the average coefficients for many channels whereas our data obtained from single-channel experiments make it possible to resolve channel-to-channel variation within the same preparation. An average Hill coefficient of 2.6 can be calculated from the individual values reported in our study.

Structural Implications of Clustered Calcium Sensitivities

The bilayer recording system has allowed us to examine the calcium dependence of the maxi K^+ channels with a

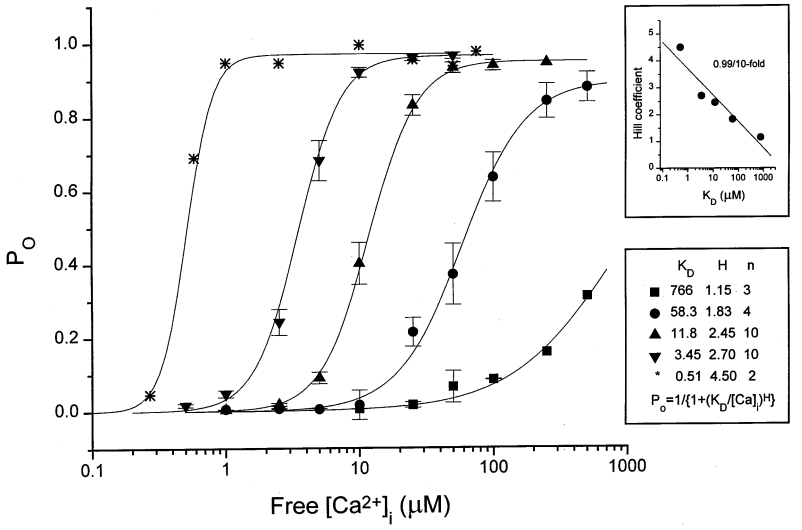

Fig. 8. Averaged open probability. Each symbol in the plot represents an average of P_o within a group and the error bars represents the standard error of the mean. The solid curve are the least-squares fit using the equation, $P_o = P_{max}/\{1 + (K/[Ca])^N\}$, where K is the equilibrium binding constant and N is the Hill coefficient. These fitted parameters and the number of trials (n) are listed in the *lower inset* of the figure. In the *upper inset*, the fitted Hill coefficients are plotted against K_d and fitted with a linear solid line.

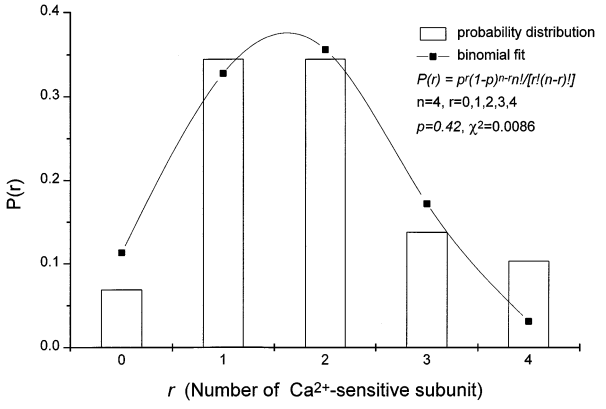

Fig. 9. Probability distribution of calcium sensitivities. $P(r)$ represents the occurring probability and the vertical bars are calculated from the number of observed channels in each calcium sensitivity group divided by the total number of recorded channels. The abscissa is the designated group number 0–4 from low to high calcium sensitivities, which corresponds to the number of putative subunits in a channel with high calcium sensitivity. The filled square connected by the solid curve are the least-squares fit with binomial distribution.

much higher resolution. From pooled calcium titration curves, we found that the distribution of the curves is clustered rather than random. The data indicate that there are only five apparent clusters generated from all our recordings. The finite number of clusters suggests that the channels can be constructed with discrete or quantized calcium sensitivities. There are two obvious ways to construct such a channel. If the gating apparatus of the channel is homo-tetrameric, then it is possible that the channel could have been modified or modulated to different levels to achieve the observed variability. However, this paradigm puts no apparent constraint on the number of clusters. If the total number of clusters (i.e., five) is not a coincidence, then it is more plausible that a hetero-tetrameric channel is formed by assembly of two distinct subunits, i.e., one with a high and the other with a low calcium sensitivity. A random combination of such a hetero-tetrameric channel is expected to comprise 0, 1, 2, 3, or 4 high calcium sensitivity subunit(s). There should be a total of only five such possible combinations for hetero-tetrameric channel construction, which is identical to the number of clusters found in our experiments.

One would expect that the occurring probability distributions for a hetero-tetrameric channel constructed from the above random mixing of two kinds of different subunits should conform to a binomial distribution. To test this, we plotted the occurring probability *vs.* the group number designated from zero to four according to the sequence of calcium sensitivities from low to high, which exactly corresponds to the presumed number of subunits in a channel with the high calcium sensitivity (Fig. 9). The filled squares connected by solid curves represents the least-squares fit of a binomial distribution to the original data shown by the bar graph. The agreement of these two distributions further supports the random mixing hypothesis. Through least-squares fitting, we have obtained the parameter $P = 0.42$ which represents the probability of selecting a putative high calcium sensitivity subunit.

We conclude from this analysis that the gating components for a maxi K^+ channel in the axian nasal gland are hetero-tetrameric and this may result from random mixing of two different subunits, one with high and the other with low calcium sensitivity. The different subunits may derive directly from alternatively spliced variants, or as a result of post-translational modifications or modulation including possible phosphorylation and dephosphorylation.

We wish to thank Jill Shuttleworth for her excellent technical assistance and helpful discussions and to Dr. Christopher Fox for his valuable advise on the statistical method in the manuscript. This work has been supported by a Postdoctoral Fellowship Award to JVW from the American Heart Association (New York Affiliate), a grant (GM-40457) to TJS from the National Institutes of Health and by Council for Tobacco Research grant SA029 to PS.

References

Adair, G.S. 1925. The Hemoglobin System. VI. The oxygen dissociation curve of hemoglobin. *J. Biol. Chem.* **63:**529–545

Brown, P.D., Loo, D.D., Wright, E.M. 1988. Ca^{2+}-activated K^+ channels in the apical membrane of Necturus choroid plexus. *J. Membrane Biol.* **105:**207–219

Egan, T.M., Dagan, D., Levitan, I.B. 1993. Properties and modulation of a calcium-activated potassium channel in rat olfactory bulb neurons. *J. Neurophysiol.* **69:**1433–1442

DiChiara, T.J., Reinhart, P.H. 1995. Distinct effects of Ca^{2+} and voltage on the activation and deactivation of cloned Ca^{2+}-activated K^+ channels. *J. Physiol.* **489:**403–418

Ernst, S.A., Ellis, R.A. 1969. The development of surface specialization in the secretory epithelium of the avian salt gland in response to osmotic stress. *J. Cell. Biol.* **40:**305–321

Furuya, K., Enomoto, K., Furuya, S., Yamagishi, S., Edwards, C., Oka, T. 1989. Single calcium-activated potassium channel in cultured mammary epithelial cells. *Pfluegers Arch.* **414:**118–124

Henderson, R.M., Cuthbert, A.W. 1991. A high-conductance Ca^{2+}-activated K^+ channel in cultured human eccrine sweat gland cells. *Pfluegers Arch.* **418:**271–275

Hill, A.V. 1921. The interactions of oxygen, acid, and CO_2 in blood. *J. Biol. Chem.* **Ii:**359–364

James, A.F., Okada, Y. 1994. Maxi K^+ channels from the apical membranes of rabbit oviduct epithelial cells. *J. Membrane Biol.* **137:**109–118

Lagrutta, A., Shen, K.Z., North, R.A., Adelman, J.P. 1994. Functional differences among alternatively spliced variants of Slowpoke, a Drosophila calcium-activated potassium channel. *J. Biol. Chem.* **269:**20347–20351

Latorre, R., Miller, C. 1983. Conduction and selectivity in potassium channels. *J. Membrane Biol.* **71:**11–30

Martin, S.C., Shuttleworth, T.J. 1994. Ca^{2+} influx drives agonist-activated $[Ca^{2+}]_I$ oscillations in an exocrine cell. *FEBS Lett.* **352:**32–36

McManus, O.B. 1991. Calcium-activated potassium channels: regulation by calcium. *J. Bioenerg. Biomembr.* **23:**537–560

Moczydlowski E., Latorre R. 1983. Gating Kinetics of Ca^{2+}-activated K^+ channels from rat muscle incorporated into planar lipid bilayers. Evidence for two voltage-dependent Ca^{2+} binding reactions. *J. Gen. Physiol.* **82:**511–542

Petersen, O.H. 1986. Calcium-activated potassium channels and fluid secretion by exocrine glands. *Am. J. Physiol.* **251**(Pt 1):G1–13

Reinhart, P.H., Levitan, I.B. 1995. Kinase and phosphatase activities intimately associated with a reconstituted calcium-dependent potassium channel. *J. Neurosci.* **15:**4572–9

Richards, N.W., Lowy, R.J., Ernst, S.A., Dawson, D.C. 1989. Two K^+ channel types, muscarinic agonist-activated and inwardly rectifying, in a Cl^- secretory epithelium: the avian salt gland. *J. Gen. Physiol.* **93:**1171–1194

Schlatter, E., Bleich, M., Hirsch, J., Markstahler, U., Frobe, U., Greger, R. 1993. Cation specificity and pharmacological properties of the Ca^{2+}-dependent K^+ channel of rat cortical collecting ducts. *Pfluegers Arch.* **422:**481–491

Segal, Y., Reuss, L. 1990. $Ba2^+$, TEA^+, and quinine effects on apical membrane K^+ conductance and maxi K^+ channels in gallbladder epithelium. *Am. J. Physiol.* **259**(Pt 1):C56–C68

Shen, K.Z., Lagrutta, A., Davies, N.W., Standen, N.B., Adelman, J.P., North, R.A. 1994. Tetraethylammonium block of Slowpoke calcium-activated potassium channels expressed in *Xenopus* oocytes: evidence for tetrameric channel formation. *Pfluegers Arch.* **426:**440–445

Shuttleworth, T.J., Thompson, J.L. 1989. Intracellular $[Ca^{2+}]$ and inositol phosphates in avian nasal gland cells. *Am. J. Physiol.* **257:**C1020–C1029

Tseng-Crank, J.C., Tseng, G.N., Schwartz, A., Tanouye, M.A. 1990. Molecular cloning and functional expression of a potassium channel cDNA isolated from a rat cardiac library. *FEBS. Lett.* **268:**63–68

Turnheim, K., Costantin, J., Chan, S., Schultz, S.G. 1989. Reconstitution of a calcium-activated potassium channel in basolateral membranes of rabbit colonocytes into planar lipid bilayers. *J. Membrane Biol.* **112:247–254**

Wei, A., Covarrubias, M., Butler, A., Baker, K., Pak, M., Salkoff, L. 1990. K^+ current diversity is produced by an extended gene family conserved in Drosophila and mouse. *Science* **248:**599–603

Wu, J.V., Shuttleworth, T.J., Stampe, P. 1996. Grouped calcium titration curves: gating components of calcium-activated K^+ channels may be heterotetramerous. *Biophys. J.* **70:**192a